

Supplementary information

Videos provided are simulation results of phases at statepoints mentioned below using method described in model and methods section of the paper.

Video #1: Phase A at $\alpha_0 = 0.2$ and $F_{active} = 100$

Video #2: Phase B at $\alpha_0 = 0.35$ and $F_{active} = 300$

Video #3: Phase C at $\alpha_0 = 0.5$ and $F_{active} = 40$

Video #4: Phase E at $\alpha_0 = 0.45$ and $F_{active} = 40$

Video #5: Phase F at $\alpha_0 = 0.65$ and $F_{active} = 100$

Video #6: Phase G at $\alpha_0 = 0.85$ and $F_{active} = 40$

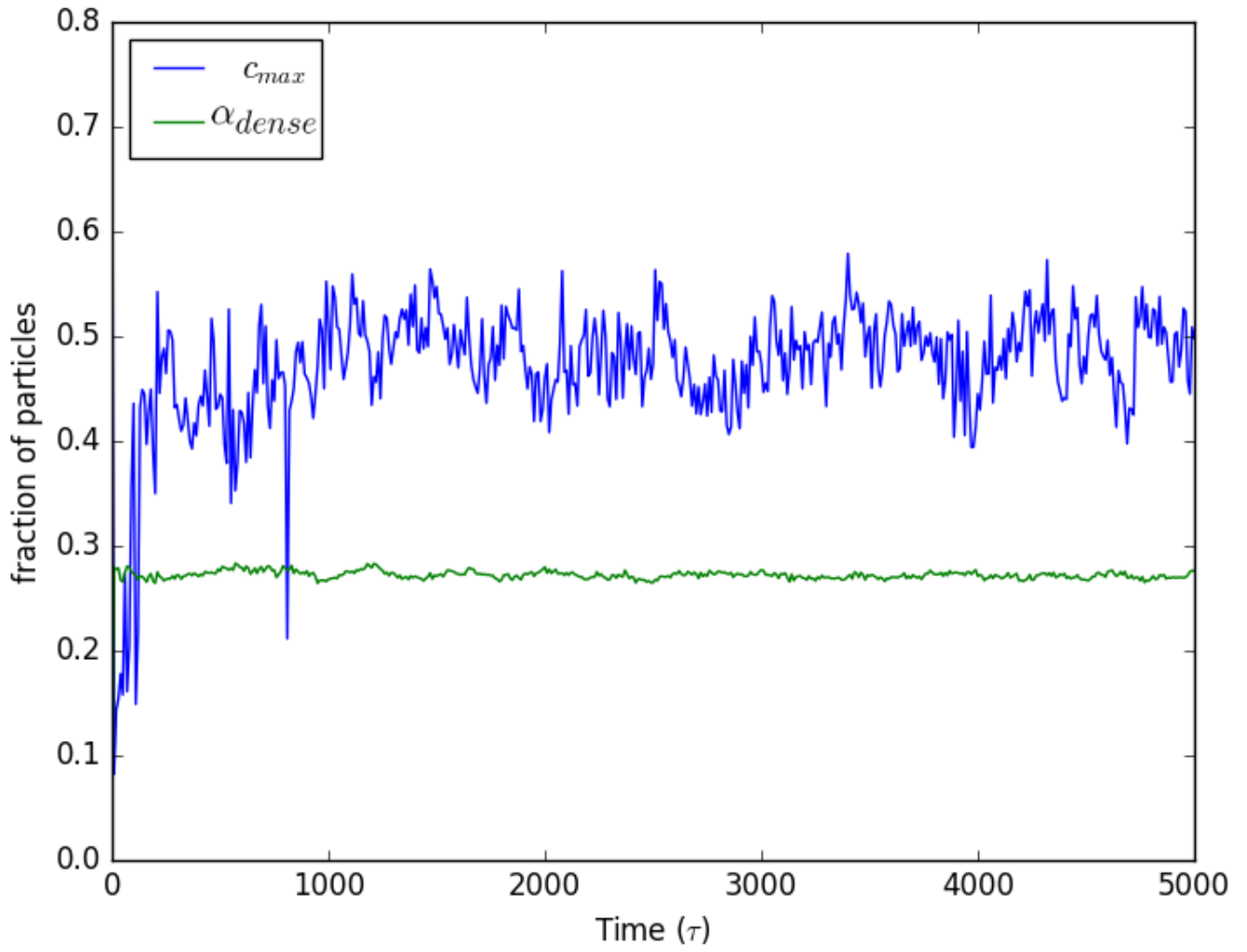


Figure 1: Time evolution of maximum cluster size, c_{max} , and fraction of CAPs, α_{dense} , in the dense phase at $\phi = 0.6$, $F_{active} = 40$, and $\alpha_0 = 0.25$.

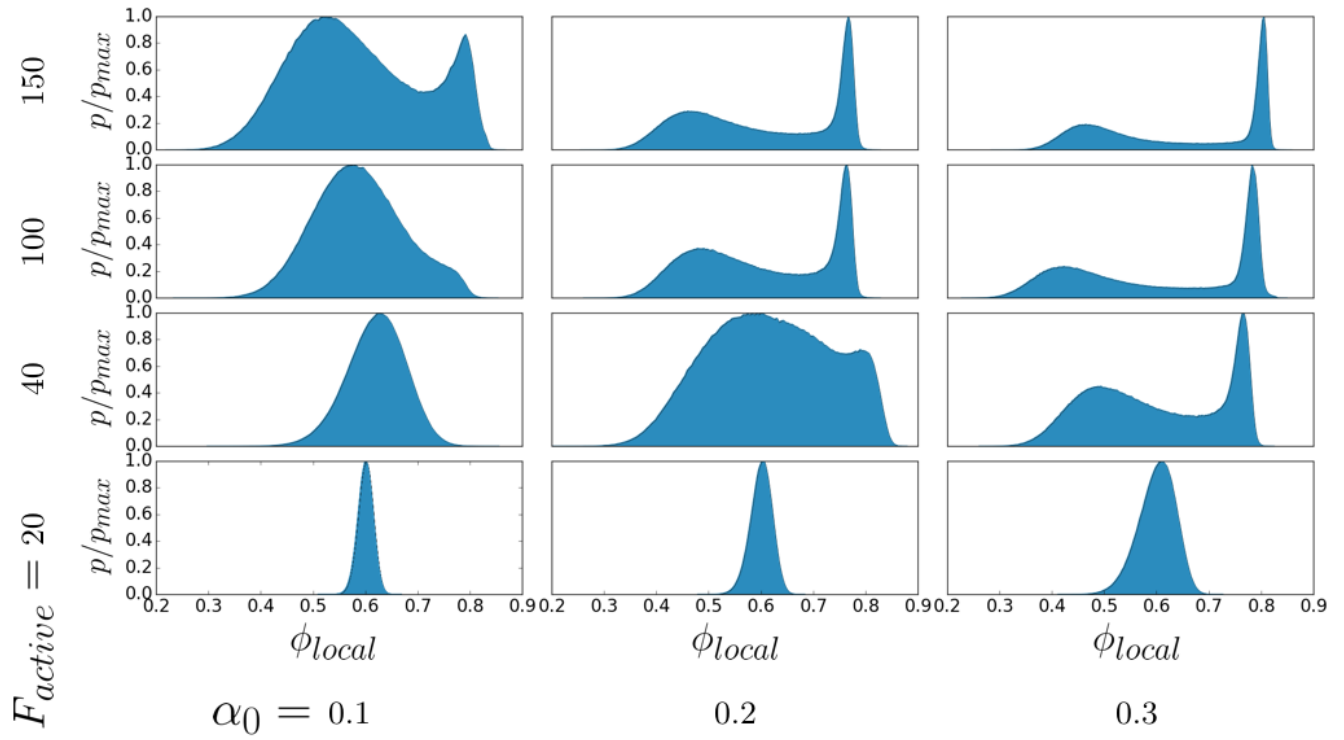


Figure 2: The density distribution of the system at $\phi = 0.6$ for varying α_0 and F_{active} . For subplots, the x-axis varies the packing fraction ϕ and the y-axis plots its probability p . The distribution is calculated at the steady state and averaged over 250 frames.

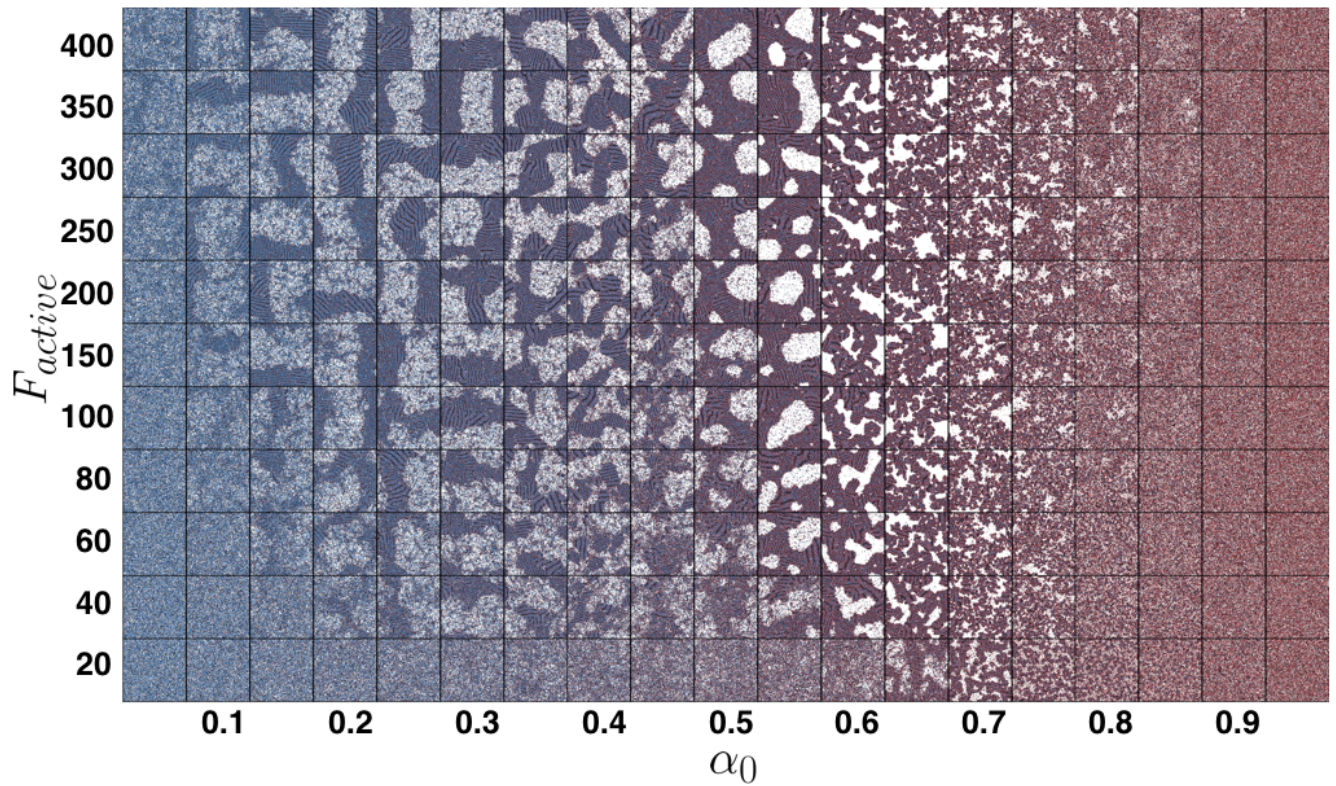


Figure 3: The phase diagram of the system at $\phi = 0.6$. The x-axis varies α_0 and y-axis varies F_{active} . Each grid point is a snapshot of the corresponding statepoint at steady state. The simulation method is described in the model and methods section of the paper.

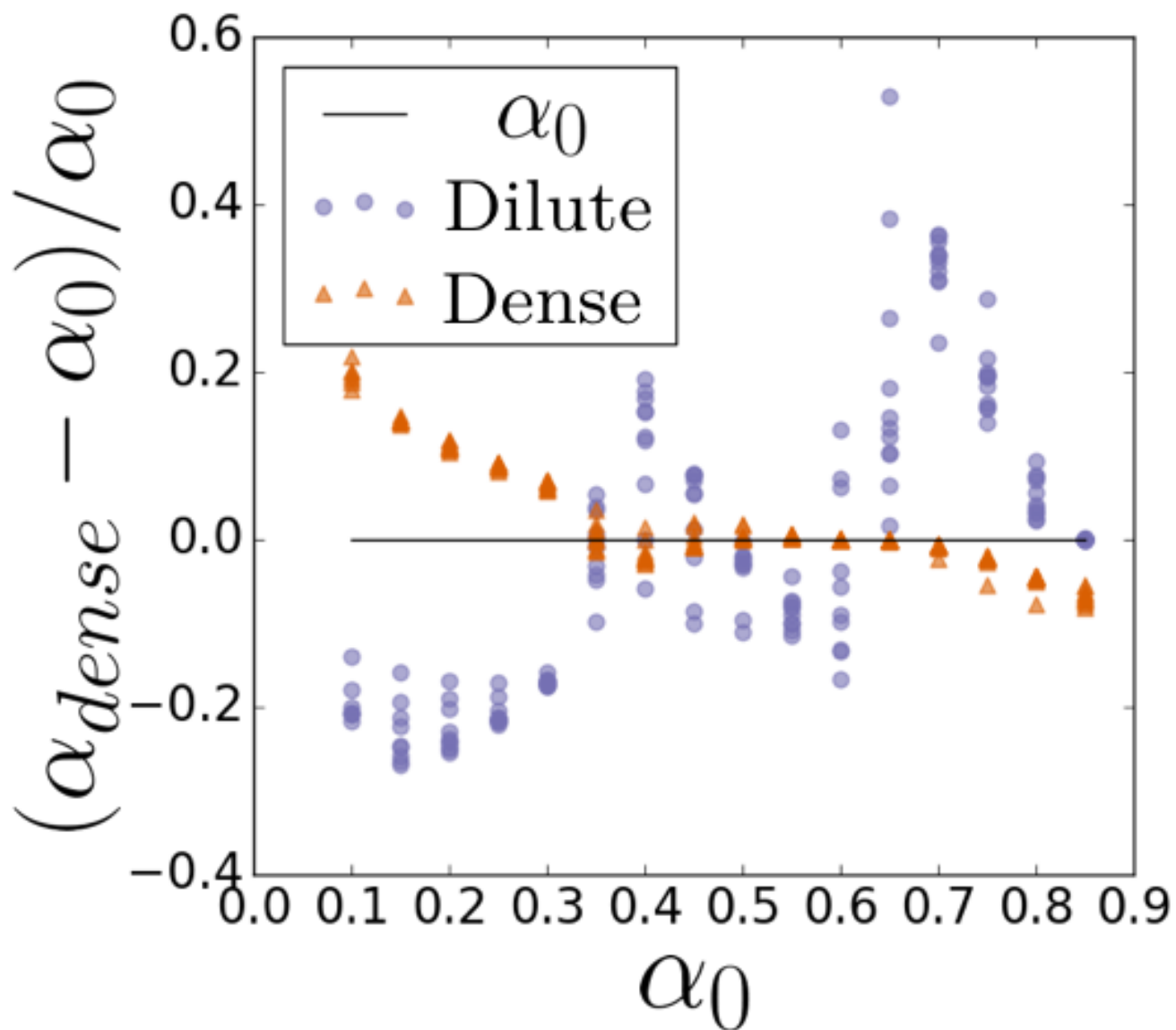


Figure 4: Fraction of CAPs in the dense and dilute phases, α_{dense} and α_{dilute} , relative to α_0 for all the state points (varying F_{active} and α_0) at $\phi = 0.6$ that phase separate and reach steady state.

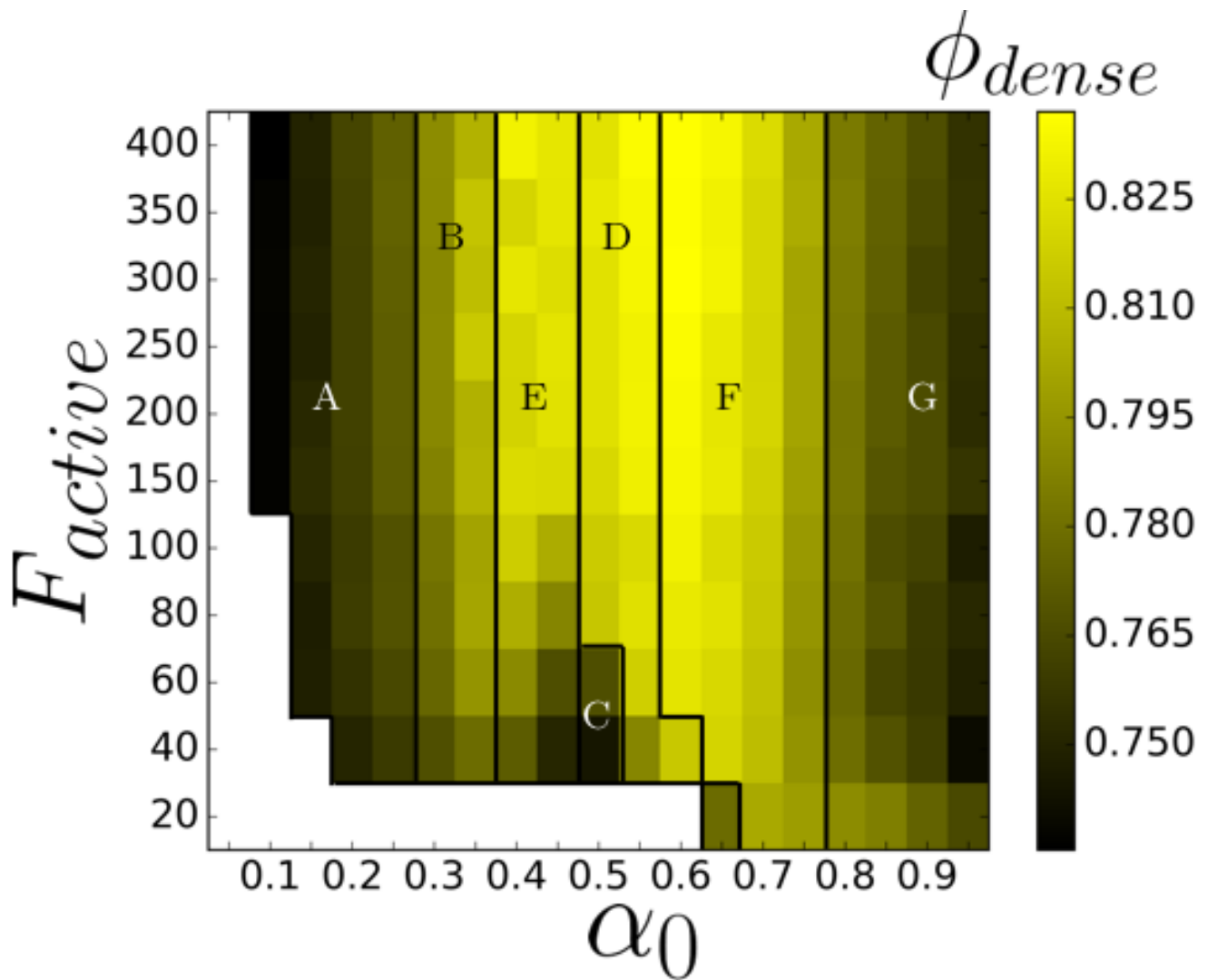


Figure 5: Heatmap of average local density, ϕ_{dense} , of the dense phase at $\phi = 0.6$, averaged over 20 frames.

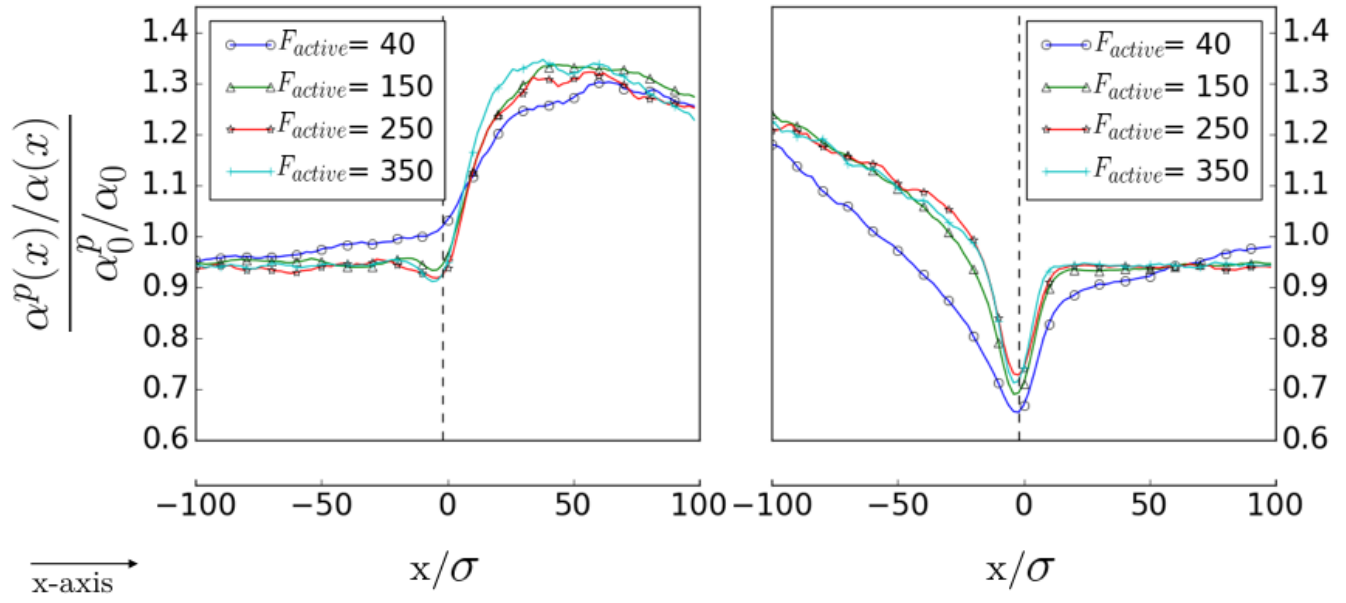


Figure 6: Ratio of passive particles to CAPs as a function of x-axis at $\alpha_0 = 0.2$, averaged over 150 frames.